

# Physiological traits associated with recent advances in yield of Chinese wheat

Bangwei Zhou



Aquesta tesi doctoral està subjecta a la llicència [Reconeixement- Compartigual 3.0. Espanya de Creative Commons](https://creativecommons.org/licenses/by-sa/3.0/es/).

Esta tesis doctoral está sujeta a la licencia [Reconocimiento - Compartigual 3.0. España de Creative Commons](https://creativecommons.org/licenses/by-sa/3.0/es/).

This doctoral thesis is licensed under the [Creative Commons Attribution-ShareAlike 3.0. Spain License](https://creativecommons.org/licenses/by-sa/3.0/es/).

# **Physiological traits associated with recent advances in yield of Chinese wheat**

## **(Rasgos fisiológicos asociados con los recientes avances en el rendimiento del trigo chino)**

Memoria presentada por **Bangwei Zhou** para optar al título de Doctor por la Universitat de Barcelona. Este trabajo se enmarca dentro del programa de doctorado de Biología Vegetal de la Facultad de Biología de la Universitat de Barcelona. Este trabajo se ha realizado en el Departamento de Biología Vegetal de la Facultad de Biología de la Universitat de Barcelona bajo la dirección del Dr. **Josep Lluís Araus Ortega** y la Dra. **M. Dolors Serret Molins**.

Doctorando  
Bangwei Zhou

Directores de Tesis  
Dr. José Luis Araus Ortega and Dra. M. Dolors Serret Molins



# CHAPTER 5



## Low-cost assessment of wheat resistance to yellow rust through conventional RGB images<sup>a</sup>

*Bangwei Zhou, Abdelhalim Elazab, Jordi Bort, Maria Dolors Serret, Jos éLuis Araus*

*Unitat de Fisiologia Vegetal, Facultat de Biologia, Universitat de Barcelona, Av. Diagonal 645, 08028, Barcelona, Spain.*

<sup>a</sup> *Submitted to Computers and Electronics in Agriculture*



*RGB camera images from rust-infected wheat canopy (left), and the corresponding out-put images from the Breedpix 1.0 software to mark the Green fraction (right). (photo taken by J. L. Araus at Aranjuez station, 2013, Spain.*

**Abstract**

Establishing low-cost methods for stripe (yellow) rust (*Puccinia striiformis* f. sp. *tritici*) phenotyping is paramount to maintain the breeding pipeline in wheat. Twelve winter wheat genotypes were grown to test rust resistance and yield performance. Physiological traits, including leaf chlorophyll content (Chl), net photosynthesis rate ( $P_n$ ), stomatal conductance ( $g_s$ ), transpiration rate ( $E$ ) and canopy temperature depression (CTD), together with diverse color components derived from RGB images, were measured at different crop stages. Grain yield (GY) and grain yield loss index (GYLI) were assessed through comparison with the previous normal planting year. Genotypes exhibited a wide range of resistance to yellow rust, with GY reducing by a factor of 10 from the most resistant ( $7.52 \text{ Mg ha}^{-1}$ ) to the most susceptible ( $0.78 \text{ Mg ha}^{-1}$ ) genotypes. Moreover yellow rust reduced Chl and to a lesser extent,  $P_n$ , while traits related to water status were lower ( $g_s$ ) or not affected ( $E$  and CTD). The color components of Hue, Green Fraction, and Greener Fraction, combined with color bands  $a$  and  $u$  were the most effective indicators for estimation of the absolute GY and GYLI due to rust-infection. They performed better than photosynthetic and transpirative traits (Chl,  $P_n$ ,  $g_s$ ,  $E$ , CTD). Conventional digital imaging appears to be a potentially affordable approach for high-throughput phenotyping of rust resistance.

**Key words:** RGB images, yellow rust, grain yield, Hue

## 1. Introduction

Wheat stripe (yellow) rust (*Puccinia striiformis* f.sp. *tritici*) has emerged as a serious threat to wheat production in China (Chen et al., 2002; Wan et al., 2007). To date, breeding for genotypic resistance has been a relatively successful strategy worldwide to curtail the impact of yellow rust on agricultural productivity (FAO, 2014, <http://www.fao.org/news/story/zh/item/177897/icode/>). However, it requires continuous testing of germplasm in search for new sources of resistance, usually major genes (Trethowan et al., 2005; Kolmer et al., 2008). In the meantime field phenotyping for yellow rust has been performed mostly on a semi quantitative basis, using visual scales (rank) of canopy effects. However, this approach is subjective in nature, fully dependent on the training of the evaluator and not easy to standardize, which furthermore prevents its application in crop growth models aimed at assessing epidemiology and/or predict yield loss (Robert *et al.*, 2004). Summarizing the current methods can be time-consuming at the very least, if not costly in labor and/or subject to bias and inaccuracies (Araus & Cairns, 2014). Therefore, whereas high-throughput field phenotyping is perceived as a bottleneck in crop breeding (Araus and Cairns, 2014), the need to develop high throughput, albeit affordable methods for field phenotyping is paramount to maintain the breeding pipeline for yellow rust resistance active (Akfirat et al., 2010). Moreover, high-throughput techniques may also be used eventually to predict potential impact of rust on crop season.

Yellow rust affects many physiological traits in wheat, which have been reported to be closely associated with grain yield loss (Gooding et al., 2000; Singh et al., 2000; Rosewarne et al., 2006). Among them is decline in chloroplast functionality, having a reduction in leaf chlorophyll content as a symptom (Chl), which subsequently causes a reduction in green leaf area index (Kuckenberg et al., 2009) and a decrease in the photosynthesis rate ( $P_n$ ) (Robert et al., 2005). Moreover, because yellow rust may also affect stomatal conductance ( $g_s$ ) and the transpiration rate ( $E$ ) of leaves (Zeng and Luo, 2008), measurement of either the  $g_s$  on individual leaves or larger-scale approaches such as measuring canopy temperature depression (CTD) have also been proposed (Devadas et al., 2009; Teena and Manickavasagan, 2014). Therefore, the potential impact of yellow rust on wheat and other crops may be predicted through the assessment of the green canopy area, the  $P_n$ , leaf Chl and eventually  $g_s$ ,  $E$  and/or CTD.

However, while  $P_n$  and  $g_s$  measured on individual leaves have the implicit limitation of being time consuming, which prevents their adoption for large-scale phenotyping (Munns et al., 2010), canopy temperature remains as an alternative providing that wheat is affected by rust (Lenthe et al., 2007; Smith et al., 1986). However to date the most promising methods for diagnosis of rust disease symptoms in wheat involve hyperspectral measurements of the reflected radiation and further process through different approaches such as neural networks (Moshou et al., 2004) or the formulation of vegetation indices (Franke et al., 2005; Ashourloo et al., 2014). However these methods are implicitly expensive, requiring either a spectroradiometer or a multispectral or hyperspectral camera, and to date, besides some exceptions (Moshou et al., 2004), they have been mostly applied at the leaf (rather than at the canopy) level (Fiorani et al., 2012).

As an alternative, the use of conventional digital images to derive green vegetation indices to predict yield and resistance to biotic stresses (caused by pests and diseases) has been reported in recent years (Diéguez-Uribeondo et al., 2003; Graeff et al., 2006; Mirik et al., 2006). Thus the low cost of red, green, blue (RGB) digital cameras makes them an attractive alternative for applications in precision agriculture and/or high-throughput phenotyping (Reyniers et al., 2004; Cabrera-Bosquet et al., 2012). Computerized digital-image analysis is a nondestructive method that can capture, process, and analyze information from digital images to estimate color parameters and vegetation indices that are able to assess the effect of stress conditions on canopy coverage, color change and grain yield (GY) in different species including wheat (Casadesús et al., 2007; Casadesús and Villegas 2014). Relevant to our study, some of the previous work using vegetation indices derived from digital RGB images has included the evaluation of plant and crop senescence caused by biotic stresses such as insect pests like greenbugs and wheat aphids (Mirik et al., 2006; Yang et al., 2009).

The information contained in a digital image includes the amount of red, green, and blue light captured by each pixel. These images can be processed by specialized (although low-cost or even open source) software, to convert RGB values directly to hue-saturation-intensity (HSI) values, which are based on human perception of color. Each component from color space can supply a range of parameters that are of potential use as indicators of agro physiological traits (Pan et al., 2007). In HSI color

space, the Hue ( $H$ ) component describes the color itself traversing the visible spectrum in the form of an angle between  $0^\circ$  to  $360^\circ$ , where  $0^\circ$  means red,  $60^\circ$  means yellow,  $120^\circ$  means green and  $180^\circ$  means cyan. Because a color parameter closely matches spectral wavelength, the  $H$  of most wheat images has been found to range between  $60^\circ$  (yellowish) and  $120^\circ$  (green) (Casades ús et al., 2007). Moreover,  $L^*a^*b^*$  (CIELab) and  $L^*u^*v^*$  (CIELuv) are two uniform color spaces recommended by the International Commission on Illumination (CIE, from the French name Commission Internationale de l'Éclairage). In the CIELab color space model, dimension  $L$ , informs on lightness, and the green to red range is expressed by the  $a$  component, with a more positive value representing a more pure red, and conversely a more negative indicating a greener color. Similarly, in the CIELuv color space model, dimensions  $u$  and  $v$  are perceptually uniform coordinates, where the visible spectrum starts with blue at the bottom of the space, moving through green in the upper left (larger scaled by  $v$ ) and out to red in the upper right (larger scaled by  $u$ ). Both  $a$  and  $u$  can be treated as scalars that rate a color change from green to red, which meets the requirement of these color traits as vegetation indices at the canopy level able to distinguish between soil or senescent/dry vegetation and green biomass (Casades ús et al., 2007). Meanwhile, in CIELab color space, blue to yellow is expressed by the  $b$  component, where the more positive the value the closer it is to a pure yellow, whereas the more negative the value the closer it is to blue. The  $b$  component has been claimed to be used for the calculation of the onset of senescence because it measures scalars of the color change that best describes the typical color shifts into yellow that occur during senescence in wheat (Kipp et al., 2014). In that sense, evaluation of plant biomass and the leaf area index in response to the water regime (Casades ús et al., 2007), or the impact of diseases such as brown-spot disease in rice and powdery mildew in wheat (Graeff et al., 2006; Kurniawati et al., 2009) are examples supporting the usefulness of these color traits. However, the applications of digital image analysis by different color bands to evaluate grain yield loss and changes in related physiological traits under rust-infection have not been assayed yet.

The objective of this study was to assess the potential use of digital RGB images as a low-cost and high-throughput approach to assess wheat genotypic resistance to yellow rust under field conditions. To that end, different color components of the images were related to total GY, yield loss and several eco-physiological parameters assessed

at the leaf ( $P_n$ ,  $g_s$ ,  $E$  and Chl) and canopy (CTD) levels.

## **2. Materials and methods**

### ***2.1 Field plots and yellow rust stress infestation***

Twelve winter wheat (*Triticum aestivum* L.) genotypes with different susceptibility to yellow rust, including 10 Chinese genotypes from Henan (cvs. Lankao 0347, Yumai 66, Aikang 58, Lankao 198, Zhoumai 18, Zhoumai 25, Lankao 298, Lankao 282, Lanakao 223 and Zhoumai 22) and 2 modern resistant Spanish cultivars (cv. Gazul and Artur Nick), were sown in the experimental field station of Aranjuez (40°03'N, 3°36'W), Madrid (Spain) from the Instituto Nacional de Investigación y Tecnología Agraria y Alimentaria (INIA) during the crop period 2012-2013. The experiment was carried out in a completely randomized block design with three replications, and each plot consisted of eight rows, seven meters in length and 0.2 m apart. Seeds were sown on 11<sup>th</sup> of November 2012 and planting density was 400 seeds m<sup>-2</sup>, resembling the usual practice at Henan. The soil type was a clay loam soil combined with high organic matter and was slightly alkaline (PH=8.1). Before sowing, 400 kg ha<sup>-1</sup> of a NPK complex fertilizer (15-15-15) was applied. At the end of tillering the plants were top-dressed with nitrogen, using a dose of 150 kg ha<sup>-1</sup> of urea (46%). A net with a mesh size of approximately 15 x 15 cm was used to prevent kernel loss by birds during grain filling. The accumulated precipitation from planting to the middle of June was 332 mm. The precipitation occurred on 61 days, and most of the continuous rains were concentrated during the whole of March, early and late April and the middle of May (Figure S1, Supporting Information). Sprinkler irrigation was provided at booting, heading and anthesis with two irrigations in April and another in early May, totaling about 180 mm. This high water input together with mild temperatures during the whole of March, late April and middle of May and high relative humidity (unusual for the time of the year) and the occurrence in Spain of the Warrior race group (GRRC, 2014) were the main causes of the severe yellow rust attack that occurred during the reproductive stage. Grains from the entire plots were harvested by machine at maturity on 12<sup>th</sup> of July 2013, and then oven-dried to 60 °C for 48 hours. Grain yield (GY) was then estimated.

## 2.2 Yellow rust impact

The impact of yellow rust in terms of grain yield loss was estimated by taking as a reference the GY achieved in the previous year (2011-2012 season) by the same genotypes in the same station with a similar experimental design and agronomical practices. Moreover, the accumulated precipitation from plating to the middle of June was only 184.5 mm, and it was mostly received during April and May, but without continuous rains (Figure S1). In addition, 360 mm of irrigation was provided at booting, heading and grain filling stages. Mean temperatures were higher in May than in the 2012-2013 crop season and no evidence of pests, diseases, water or nutrient stress were apparent. Therefore, the GY achieved during this season represented the usual values achievable under good agronomical conditions in the area.

The grain yield loss index (GYLI) (which could be considered as a yellow rust stress index) was calculated for each genotype as follows:

$$\text{Grain yield loss index} = \frac{\text{Grain yield (2012)} - \text{Grain yield (2013)}}{\text{Grain yield (2012)}} * 100$$

Here: grain yield (2012) represents the average GY for a given genotype in the optimal 2011-2012 crop season and grain yield (2013) represents the GY achievement for each plot of this particular genotype in the 2012-2013 season.

## 2.3 Photosynthetic and transpirative gas exchange and canopy temperature depression

An infrared gas analyzer (Li-6400 system, Li-Cor, Inc., Lincoln, NE, USA) was used to measure net photosynthesis ( $P_n$ ), stomatal conductance ( $g_s$ ) and transpiration rate ( $E$ ) in the middle portion of the flag leaf blade, avoiding wherever possible evident fungal lesions. Measurements were performed about two weeks after anthesis, when yellow rust was fully spread at the canopy level. Measurements took place between 10:00 to 14:00 on a sunny day. The gas exchange chamber was maintained at 25 °C, 50% of relative humidity, 400  $\mu\text{mol mol}^{-1}$  of  $[\text{CO}_2]$  and a PPFD of 1200  $\mu\text{mol m}^{-2} \text{s}^{-1}$ . Chlorophyll content (Chl) was measured at the bottom, middle and tip parts of five flag leaf blades per plot, using a portable meter (Minolta SPAD 520 Meter, Plainfield, IL, USA) avoiding fungal lesions. Measurements were performed at jointing, heading and grain filling, the last date on the same day as the gas exchange measurements. In

addition, canopy temperature depression (CTD) was measured as  $CTD = T_a - T_c$ , where  $T_a$  and  $T_c$  were the air temperature and canopy temperature for each plot, respectively. Air temperature was measured with a Testo 635 humidity/temperature measuring instrument (Testo AG, Lenzkirch, Germany), whereas canopy temperature was derived from thermal images obtained by an infrared camera (Midas 320L Dias Infrared GmbH, Germany), which has a spectral range of 8-14  $\mu\text{m}$  and produces pictures with a spatial resolution of  $320 \times 240$  pixels. Measurements were carried out between 10:00 and 14:00 h on the same day as the gas exchange measurements. One thermal image was taken for each single plot, the camera operator always standing 1.5 m away from each plot, with the sun placed behind and capturing the opposite border of the plot in the center of the image.

#### ***2.4 Digital image acquisition and analysis***

A single digital picture per plot was obtained using a Nikon D7000 camera with a focal length of 18 mm, placed in a zenithal position, about 60 cm above the canopy. Measurements were performed at jointing, heading and two weeks after anthesis; the last one coinciding with the gas-exchange measurement. Shutter speed was set at 1/250 and the aperture and ISO sensitivity were left automatic. Digital pictures (of about 4 megapixels resolution) were saved as JPEG format.

All the color parameters were analyzed with the BreedPix version 1.0 tool as described elsewhere (Casadesús et al., 2007) run under Java Advanced Imaging functions (Sun Microsystems Inc., Santa Clara, CA, USA), which is a free-access software designed to analyze hundreds of pictures simultaneously in a fast manner, delivering a number of indices as output. In the current work, the images of bare soil and the wheat canopies taken at jointing, heading and grain filling were primarily differentiated from red, green and blue (RGB) color space, and the resulting coordinates were directly converted to other groups of color parameters by the software. For an easier interpretation, RGB values were converted by using the BreedPix functions to hue-saturation-intensity (HSI) values, which are based on human perception of color. Simultaneously, chromaticity coordinates from CIELab and CIELuv color spaces were calculated as in Trussell et al. (2005). Beside the diverse color parameters, for each original image, two derived images were produced

with gray pixels representing the background and green pixels representing plant parts. One derived image was obtained from the color parameter “green fraction” ( $GF$ ) and the other derived image from the “greener fraction” ( $GGF$ ) (Casadesús and Villegas, 2014) (Figure 1). The  $GF$  corresponds to the proportion of green pixels in an entire image, where a pixel is considered green if its Hue value is within the range  $60^{\circ}$ – $180^{\circ}$ . The  $GGF$  was aimed at quantifying the fraction of fully functional green cover, excluding yellowish pixels that may correspond to senescent leaves, and was calculated as the proportion of pixels whose Hue value is within the range  $80^{\circ}$ – $180^{\circ}$ .

## **2.5 Statistical analyses**

In order to evaluate the genotypic susceptibility to yellow rust in terms of absolute grain yield, yield loss, gas exchange, chlorophyll content and the different color parameters derived from the RGB images, analysis of variance (ANOVA) was performed using the general linear model procedure. Mean separation of genotypes for the analyzed parameters was done by a Tukey-b’s multiple comparison test ( $P < 0.05$ ). Pearson correlations were performed between the color parameters and the yield and physiological parameters. The datasets were subjected to principal component analysis using the correlation matrix in order to standardize each variable and a Varimax rotation was applied to aid interpretation of the parameters. All the data were analyzed using the SPSS v.16 statistical package (SPSS Inc., Chicago, IL, USA), and figures were drawn using SigmaPlot 12.5 for Windows (Sysat Software Inc., Point Richmond, CA, USA).

## **3. Results**

### **3.1 Grain yield, grain yield loss and physiological traits**

Under the yellow rust infected conditions of the 2012-2013 crop season a wide range of genotypic variability existed for grain yield (GY), as well as for the grain-yield loss index (GYLI). The former ranged from less than  $1 \text{ Mg ha}^{-1}$  (Lankao 298) to over  $7 \text{ Mg ha}^{-1}$  (Zhoumai 22), while the latter ranged from about -3% to 90% (Table 1). By contrast, under the non-stress field condition of the 2011-2012 season, there was also

genotypic variability, but the range of GY was much narrower (from 5 to slightly beyond 8 Mg ha<sup>-1</sup>).

Genotypic variability also existed for the leaf chlorophyll content (Chl) measured at jointing and heading, but it strongly increased during grain filling, coinciding with the spreading of the yellow rust (Table 1). Net photosynthesis ( $P_n$ ), stomatal conductance ( $g_s$ ) and transpiration rate ( $E$ ) during grain filling also exhibited genotypic variability, whereas canopy temperature (CTD) did not. Nevertheless, a positive correlation existed between CTD and leaf  $E$ , the two traits informing on transpiration (Table 2).

Whereas genotypic values of GY for the two consecutive crop seasons were positively correlated. GY of the rust-affected season (2012-2013) was highly and negatively correlated with GYLI (Table 2).  $P_n$ , and to a lesser extent  $g_s$  and  $E$ , correlated negatively with GYLI, whereas  $P_n$  was the only physiological trait (positively) correlated with GY. CTD did not correlate with either GY or GYLI.



Figure 1. RGB camera images (upper) from bare soil (left), wheat canopy at jointing (center) and rust-infected wheat canopy at grain filling (right, two weeks after anthesis), and the corresponding out-put images from the Breedpix 1.0 software to mark the Green fraction (*GF*) (middle) and Greener fraction (*GGF*) (bottom).

	GY	GY	GYLI	Chl			P <sub>n</sub>	g <sub>s</sub>	E	CTD
	(rust infested)	(normal)		Jointing	Heading	Post-anthesis				
	(Mg ha <sup>-1</sup> )		(%)				mmol m <sup>-2</sup> s <sup>-1</sup>	mol m <sup>-2</sup> s <sup>-1</sup>	mmol m <sup>-2</sup> s <sup>-1</sup>	(°C)
Lankao 298	0.78 f	7.03 abc	88.91 a	44.7 cd	46.6 bc	31.0 e	20.1 bc	0.31 bc	6.6 bc	5.7
Lankao 198	1.50 e	7.04 abc	78.69 a	44.0 cd	48.5 abc	37.7 d	20.2 bc	0.31 bc	6.7 bc	6.2
Lankao 282	1.78 de	6.07 bcd	69.91 ab	46.7 bc	53.0 ab	45.0 c	18.4 c	0.33 bc	6.9 abc	6.7
Lankao 223	2.95 d	5.48 cd	46.15 cd	46.5 bc	50.6 abc	48.2 c	23.3 abc	0.37 abc	7.6 abc	7.2
Aikang 58	2.99 d	6.30 bcd	52.56 bc	50.2 ab	47.3 abc	50.0 bc	24.4 ab	0.43 a	8.4 a	6.3
Yumai 66	3.09 d	5.00 c	37.25 cde	52.2 a	51.6 ab	57.4 a	23.8 ab	0.39 ab	7.8 ab	7.1
Zhoumai 25	3.89 d	6.13 bcd	34.13 cde	46.3 bc	49.9 abc	45.6 c	24.0 ab	0.37 abc	7.8 ab	6.4
Lankao 0347	4.85 c	6.19 bcd	21.71 ef	49.9 ab	47.6 abc	51.4 abc	21.6 abc	0.43 a	8.4 a	7.1
Gazul (SG)	5.28 c	7.80 ab	32.33 cde	41.4 d	44.0 c	48.0 c	25.0 ab	0.35 abc	7.3 abc	6.5
Arthur Nick(SG)	6.23 b	8.38 a	25.65 de	41.1 d	53.7 a	44.7 c	20.9 abc	0.29 c	6.2 c	6.3
Zhoumai 18	6.71 b	7.69 ab	12.65 ef	42.2 cd	46.7 bc	48.2 c	23.8 ab	0.41 ab	8.1 ab	7.3
Zhoumai 22	7.52 a	7.28 ab	-3.59 f	43.3 cd	49.3 abc	55.2 ab	26.0 a	0.38 abc	7.7 abc	6.3
Mean	3.96	6.7	41.6	45.72	49.06	46.86	22.6	0.37	7.5	6.6
Genotypes	154.76***	33.2***	22976***	431.0***	268.8**	1687.2***	178.3***	0.07***	17.2***	8.0

Table 1. Mean value and sum of squares combined with analysis of variance for a set of agronomical and physiological traits measured in a set of twelve wheat genotypes suffering yellow rust infection during grain filling in the cropping season 2012-2013.<sup>1</sup>

<sup>1</sup> The agronomical traits included were grain yield in the 2012-2013 cropping season (GY rust infected), reference grain yield (GY normal) taken as the yield of the same genotypes under similar agronomical condition but without suffering yellow rust infection (yield at the same station in the season 2011- 2012) and the grain yield loss index (GYLI). Physiological traits were measured in the 2012-2013 crop season and included chlorophyll content (Chl, SPAD value) of the last fully expanded leaf blade at jointing, heading and grain filling, as well as net photosynthesis (P<sub>n</sub>), stomatal conductance (g<sub>s</sub>) and transpiration rate (E) of the flag leaf blade during grain filling and the canopy temperature depression (CTD) measured during grain filling. The values are the means of 3 plots per genotype. (SG, Spanish genotype; \*\*, P ≤ 0.01 and \*\*\*, P ≤ 0.001).

	GY (rust infested)	GY (normal)	GYLI	P <sub>n</sub>	g <sub>s</sub>	E
GY (normal)	0.45**					
GYLI	-0.94***	-0.12				
P <sub>n</sub>	0.47**	-0.10	-0.57***			
g <sub>s</sub>	0.26	-0.28	-0.40*	0.69***		
E	0.26	-0.28	-0.41*	0.58***	0.95***	
CTD	0.19	-0.15	-0.27	0.20	0.54**	0.61***

Table 2. Pearson correlation coefficients among grain yield for the rust-infected trial in the 2012-2013 crop season (GY rust infested), grain yield for the same genotypes without stress in the 2011-2012 crop season (GY normal), grain yield loss index (GYLI), and the different physiological traits. Footnote<sup>2</sup>

### 3.2 Color parameter variation

Different color parameters and vegetation indices derived from digital RGB images were measured at jointing, heading and grain filling (Table 3). Genotypic variability for most of these parameters was absent at jointing but appeared at heading and was maximal during grain filling, coinciding with the burst in yellow rust. Thus for each color component from the IHS, CIELab and CIELuv spaces, there were no genotypic differences in the color distribution from canopy images at jointing. By contrast at heading, the color parameters *H*, *S*, *a*, *b*, *u* and *v* and the vegetation index *GF* exhibited significant genotypic differences. During grain filling these color parameters increased their genotypic significance, and both vegetation indices (*GF* and *GGF*) exhibited genotypic significance. By contrast, the parameters *I* and *L* did not exhibit genotypic differences at any time during the crop cycle (Table 3; Table S1).

<sup>2</sup> Net photosynthesis rate (P<sub>n</sub>), stomatal conductance (g<sub>s</sub>), the transpiration rate (*E*) of the flag leaf blade, and the canopy temperature depression (CTD) measured during grain filling in the 2012-2013 crop season. Correlations were calculated across the whole set of genotypes and replicates (\*, P ≤ 0.05; \*\*, P ≤ 0.01 and \*\*\*, P ≤ 0.001, n = 36).

	Bare Soil		Jointing			Heading			Grain filling (rust infected)		
	Mean	SE	Mean	SE	Genotype	Mean	SE	Genotype	Mean	SE	Genotype
<i>I</i>	0.38	0.01	0.33	0.01	0.00	0.27	0.03	0.01	0.29	0.02	0.00
<i>H</i>	34.35	5.44	83.33	4.47	292.72	111.31	11.09	3197.25***	64.08	12.50	5209.49***
<i>S</i>	0.14	0.05	0.31	0.06	0.07	0.15	0.04	0.04**	0.27	0.04	0.06***
<i>L</i>	44.22	1.70	44.80	1.20	18.17	35.03	3.87	242.38	36.73	1.84	38.95
<i>a</i>	0.05	1.64	-19.73	1.52	22.20	-16.01	1.81	75.47**	-8.87	3.44	395.11***
<i>b</i>	16.16	3.47	30.88	3.99	220.48	16.94	3.06	278.08***	22.64	2.09	126.70***
<i>u</i>	8.26	3.89	-13.29	1.31	15.59	-12.32	1.74	54.71*	-1.68	4.83	786.31***
<i>v</i>	18.15	3.47	35.20	3.61	159.51	20.08	3.48	344.29***	24.23	1.78	72.88**
<i>GF</i>	0.08	0.08	0.97	0.02	0.00	0.97	0.02	0.01*	0.62	0.26	2.34***
<i>GGF</i>	0.02	0.02	0.70	0.10	0.18*	0.93	0.03	0.02	0.37	0.25	2.07***

Table 3. Mean value, standard error and sum of square type (III) for the different color parameters evaluated on the bare soil as well in the canopy at jointing, heading and during grain filling when rust infestation was already present. Footnote<sup>3</sup>

<sup>3</sup> For each crop stage, values are the mean and SE of the twelve different wheat genotypes for 36 measurements, whereas values for the bare soil are the means and SE of the three stages for 3 measurements. The color parameters represented the components of the whole image expressed in the color spaces of Intensity, Hue and Saturation (HIS), CIELab (*L*, *a* and *b*) and CIELuv (*L*, *u* and *v*). *GF* is the relative green fraction and *GGF* is the relative greener fraction from the *H* histogram in the entire image. (\*,  $P \leq 0.05$ ; \*\*,  $P \leq 0.01$  and \*\*\*,  $P \leq 0.001$ ).

### 3.3 Comparative performance of color parameters evaluating grain yield and genotypic susceptibility to rust

Principal component analysis (PCA) was performed to get a broad view of the different categories of color parameters and their association with GY at jointing, heading and grain filling (Figure 2). In the PCA corresponding to jointing, the two first components together accounted for 73% of accumulated variance. Whereas PCA showed that GY was poorly associated with color parameters, *H* was positively associated with *GGF* and negatively related to *GF*, *b*, *v* and *S*. Meanwhile, traits such as *a* and *u* were not related to *H*, but associated with *L*. At heading the two first components of the PCA accounted for 67% of total variation. Again, GY was in general poorly associated with the different color traits. The traits *v*, *b*, *S* and *GF* were located in the right side of the first component, whereas *H* was placed in the left side and *L* and *I* were sited close together in the upper part of the vertical axis, opposite to *a* and *u*, while GY was near the middle, not far from *GGF*. By contrast, during grain filling the two first components of the PCA represented nearly 82% of accumulated variation and GY was placed in the right side of the first axis, closely associated with *GGF*, *GF* and *H*, while *S*, *u* and *a* were placed opposite in the left side of the first component. The traits *I*, *L* and *v* were placed in the upper part of the second component, while *b* was placed in between the last two categories of traits.

The specific performance of the different color parameters estimating GY and GYLI was assessed through linear correlation analysis (Table 4). Color traits assessed at jointing and heading failed to correlate with GY and GYLI, whereas most of the color parameters correlated with GY and GYLI during grain filling, reflecting the wider genotypic variability in color parameters during grain filling compared with the previous phenological stages. The color parameter *H* and the vegetation indices *GF* and *GGF* were positively correlated with GY ( $r = 0.87, 0.87$  and  $0.89, P < 0.001$ , respectively), while the *a* and *u* parameters were negatively correlated with GY ( $r = -0.88$  and  $-0.87, P < 0.001$ , respectively). The parameters *S* and *b* were also negatively correlated with GY but in a weaker manner ( $r = -0.68$  and  $-0.45$ , respectively,  $P < 0.01$ ). The color components *L*, *I* and *v* did not correlate with grain yield. The pattern of correlations of the different color traits with GYLI was comparable to the correlations of these parameters with GY, with correlation coefficients having opposite signs and

slightly higher absolute values, as for the correlations with GY.

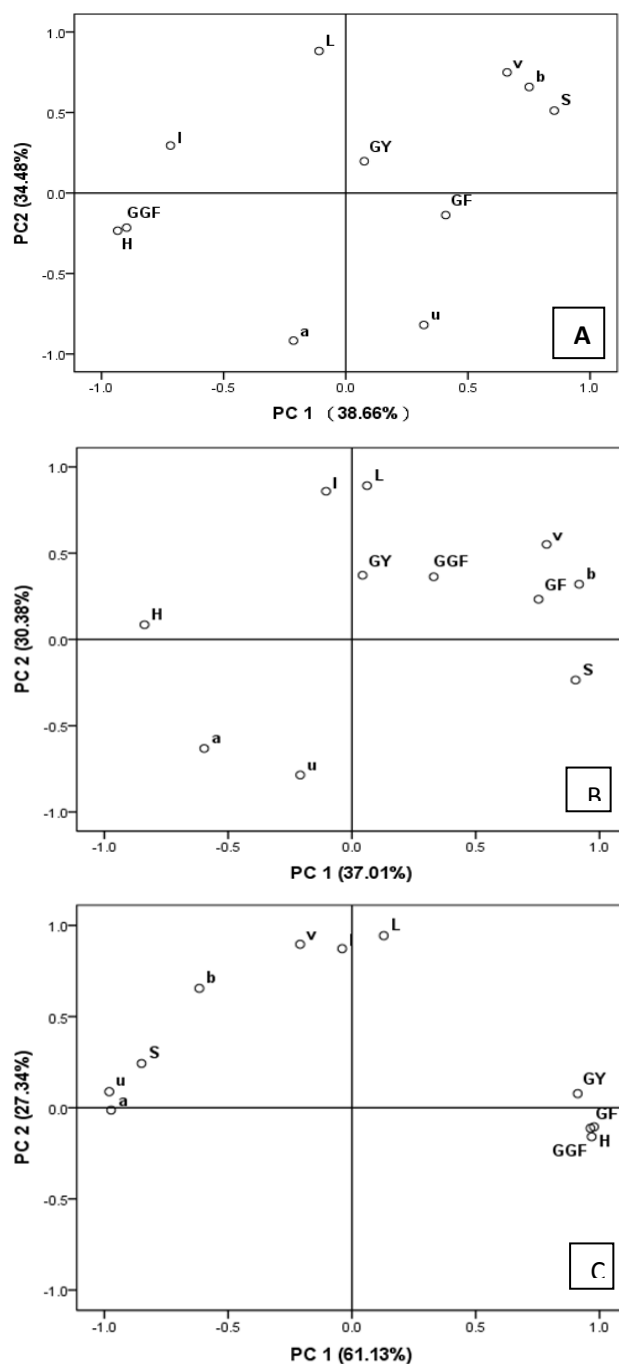


Figure 2. Principal component analysis (PCA) of color parameters and grain yield (GY) at jointing (A), heading (B) and grain filling (C) for 12 wheat genotypes suffering post-anthesis yellow rust infection. Footnote<sup>4</sup>

<sup>4</sup> The color parameters represent the average color components of the whole image expressed in the color spaces of Hue Intensity Saturation ( $H$ ,  $I$  and  $S$ ), CIELab ( $L$ ,  $a$  and  $b$ ) and CIELuv ( $L$ ,  $u$  and  $v$ ).  $GF$  is the relative green fraction and  $GGF$  the relative greener fraction of  $H$  of the image.

	GY			GYLI
	Jointing	Heading	Grain filling	Grain filling
<i>Chl</i>	—	—	-0.67**	-0.77***
<i>I</i>	0.1	0.23	-0.04	-0.04
<i>H</i>	-0.17	-0.04	0.87***	-0.86***
<i>S</i>	0.13	-0.09	-0.68***	0.72***
<i>L</i>	0.19	0.23	0.14	-0.18
<i>a</i>	-0.08	-0.12	-0.88***	0.89***
<i>b</i>	0.14	0.09	-0.45**	0.47**
<i>u</i>	0.01	-0.14	-0.87***	0.88***
<i>v</i>	0.15	0.15	-0.08	0.07
<i>GF</i>	-0.2	0.33	0.87***	-0.90***
<i>GGF</i>	-0.22	0.36*	0.89***	-0.86***

Table 4. Pearson correlation coefficients of the relationships of grain yield (GY) and grain yield loss index (GYLI) against leaf chlorophyll content (Chl) and different color parameters derived from RGB images taken at jointing, heading and two weeks after anthesis, across the set of 12 wheat genotype and 3 replicates per genotype. Footnote<sup>5</sup>.

## 4. Discussion

### 4.1 Effect of yellow rust on grain yield and photosynthetic and transpirative parameters

The set of genotypes used in this study showed a high genotypic variability for yellow-rust resistance. Some of the Chinese genotypes exhibited higher resistance to yellow rust than the Spanish checks. In fact, the genotype “Zhoumai 22” was unaffected and Zhoumai 18” slightly affected. In the case of “Zhoumai 18”, reports have indicated that it is a slightly susceptible genotype (Yin *et al.*, 2009; Han *et al.*, 2010). The genotypes “Aikang 58” and “Zhoumai 22” have been reported to have high resistance to yellow rust because they carry the *YrZH84* gene from the

<sup>5</sup> Color parameters included: Intensity hue saturation (IHS) color space and each of its components; lightness (*L*); *a* and *b* color components from CIELab; *u* and *v* color components from CIELuv; *GF*, green fraction; *GGF*, greener fraction are listed. (\*,  $P \leq 0.05$ ; \*\*,  $P \leq 0.01$  and \*\*\*,  $P \leq 0.001$ ,  $n = 36$ ).

well-known parent donor “Zhou 8425B” (Yin *et al.*, 2009). However, “Aikang 58”, exhibited moderate susceptibility to rust, which suggests that *YrZH84* alone is not conferring full resistance to the new strain of yellow rust (Yin *et al.*, 2009; He *et al.*, 2011). In general, the most productive genotypes in the absence of yellow rust (2011-2012 season) were those that still yielded more under rust attack. This is supported by the positive relationship between GY across the two crop seasons (Table 2). On the whole the modern high-yielding Chinese genotypes from Henan are characterized by a low-to-moderate susceptibility to new yellow rust strains (He *et al.*, 2011). However, in our results no relationship existed between yield potential and rust resistance as shown by the lack of relationship between GY during the 2011-2012 season and GYLI (Table 2).

The higher correlation between GY and GYLI with Chl content compared to the other physiological traits ( $P_n$ ,  $g_s$  and  $E$ , CTD) suggests that yellow rust may already reduce yield through a loss in Chl, whereas the effect of infection on  $P_n$  is smaller. In fact it is well known that susceptibility to yellow rust causes a fast senescence in leaves that is characterized by a loss in Chl content (Spitters *et al.*, 1990; Scholes and Rolfe, 1996; Devadas *et al.*, 2009). Moreover, previous studies have also found that Chl content seems more affected by leaf rust than  $P_n$ , (Berghaus and Reisener, 1985; Carretero *et al.*, 2011). Concerning the mechanism that decreases  $P_n$ , Carretero *et al.* (2011) concluded that reductions in photosynthesis were due to effects on non-stomatal processes other than the amount of nitrogen in the leaves, probably including those associated with energy capture by photosystems (reductions in chlorophyll concentration) and the electron transport rate. In that sense Robert *et al.* (2005) concluded for wheat that leaf rust has no global effect on the  $P_n$  of the symptomless parts of the leaves. Moreover, as a response to yellow rust and other fungal diseases, a set of physiological processes are triggered as a defense reaction using assimilates that otherwise would go to growth and seed production (McGrath and Pennypacker, 1990; Scholes *et al.*, 1994; Herrera-Foessel *et al.*, 2006). This may also affect  $P_n$  through an indirect mechanism. Thus it has been reported that healthy leaves from plants exposed to brown rust infection exhibited a decrease in  $P_n$  through an increase in dark respiration, whereas no effect (decrease) on  $g_s$  was reported (Bethenod *et al.*, 2001). However, at least for wheat exposed to leaf rust, additional studies have discarded the increase in dark respiration as a cause of the decrease in photosynthesis (Carreter *et*

al., 2011).

In our study the genotypic differences in  $P_n$  seem positively related to differences in  $g_s$ . McGrath and Pennypacker (1990) reported that in response to stem rust and leaf rust,  $P_n$  and  $g_s$  decreased in wheat flag leaves, but internal  $CO_2$  concentration increased. However the reduction in  $g_s$  associated with leaf rust infection in wheat is probably a consequence of the negative effect of the pathogen on the photosynthesis machinery, which leads to an increase in internal  $CO_2$  concentration, causing a subsequent decrease in  $g_s$  (Carretero et al., 2011). Overall, our study supports the concept that the negative effect of rust infection on GY was not primarily caused by a decrease in stomatal aperture. In fact, the lack of correlation of  $E$  and CTD with GY and GYLI, together with the weak (negative) correlation of  $g_s$  with GYLI, also supports a minor effect of yellow rust on GY mediated through a diminishment in  $g_s$ . Robert et al. (2005) concluded from their study linking loss in photosynthetic capacity with symptoms of leaf rust attack in wheat that the assessment of total visible diseased tissue (chlorotic plus necrotic tissues) gave the best prediction of the disease impact on host canopy photosynthesis in the field. In the same way, Carretero et al. (2011) postulated that because wheat leaf rust reduced the net photosynthesis rate at light saturation, no effects will be observed at low irradiance levels and consequently leaf rust affects light interception rather than radiation use efficiency at the crop level. Therefore, evaluating the amount of green tissues at the canopy level rather than the gas exchange of even the chlorophyll content of individual leaves seems to be the most suitable alternative to assess the effects of yellow rust.

#### ***4.2 Relationships of HIS color components with genotypic performance***

In the previous studies, the  $H$  component from HIS color space had been proposed as a useful indicator of greenness in species (e.g. wheat, turf) under different nitrogen treatments (Casades ús, et al., 2005; Karcher and Richardson, 2005). In our work, the mean value of  $H$  (83.3 °) during booting showed that canopy colors ranged across the middle of the yellowish to green bands (Table 3; Table S1). This might be due to the fact that the soil was not completely covered by the canopy because the  $H$  of bare soil is lower than a well-developed plant canopy, which may be found in the case of a healthy crop at heading (Table 3). Therefore, at jointing, exposure of the soil can

reduce the averaged canopy  $H$  to values close to yellow bands. At heading, the  $H$  value was far higher (111.3 °) reflecting the larger canopy and the healthy status of the crop. In work on durum wheat under Mediterranean conditions carried out by Casadesús et al., (2007),  $H$  values ranged between 50 ° and 110 °, reflecting the wide range of biomass and senescence status caused by a large variation in water conditions (from well irrigated to severe water stress). However, in our study the  $H$  value decreased strongly (64.1 °) during grain filling, reflecting the effect of rust infection in yellowing the leaves and culms (Römer et al., 2012).

$GF$  explains the proportion of green pixels (from 60° to 120°) to the total pixels within  $H$ , whereas  $GGF$  is more stringent and represents the proportion of pixels within the range from 80° to 120° (Lukina et al., 1999; Casadesús et al., 2007, 2014). In our study the mean values of  $GF$  (0.97) during jointing and  $GF$  (0.97) and  $GGF$  (0.93) during heading nearly reached saturation (1.0 means the image all covered by pixels within the  $GF$  or  $GGF$  categories) (Table 3). The moderate value (0.70) for  $GGF$  at jointing may be the consequence of a low Chl content of leaves due to fast growth associated with stem elongation (Arregui et al., 2006). At grain filling, both  $GF$  and  $GGF$  were very efficient at capturing genotypic differences in color changes associated with yellow rust, with genotypic means ranging from 0.09 to 0.92 and from 0.02 to 0.77, respectively.

In the HSI color space, color component  $S$  usually describes the spectral distribution of light, remaining roughly constant even as brightness and colorfulness change with different illumination (Cheng et al., 2001). Although  $S$  was linearly correlated with  $GY$  and rust resistance, correlations were less strong than those with  $GF$  and  $GGF$ . The lack of a relationship of the  $I$  component with  $GY$  and  $GYLI$  may be due to the fact this color component is used to mask shadows, which is a common problem in ground photography acquisition (Pan et al., 2007).

### ***4.3 Relationships of CIELab and CIELuv color components with genotypic performance***

In the CIELab and CIELuv color spaces, both  $a$  and  $u$  can be treated as scalars that represent colors between the extremes of red and green, which are also independent of

blue bands, and hence it can be assumed that they are unaffected by any cyan/bluish features in the scene (Casadesús et al., 2005). Similar to  $H$ , the sensitivity of  $a$  and  $u$  to red colors means that they can be affected by soil color when plants do not entirely cover the soil (Casadesús et al., 2007). However, the high strength of the relationships between  $a$  and  $u$  with GY and GYLI (Table 4) reflects the capacity of these color traits to capture changes in green color associated to rust infection (Graeff et al., 2006). In the case of the color parameters  $b$  and  $v$ , they were not suitable color bands to estimate GY and GYLI as shown by the weak ( $b$ ) or lack of correlation ( $v$ ) of these traits (Table 4). Concerning the color parameter  $L$ , it represents the camera's self-adjustment to the images, thus making it unsuitable to estimate the effect of yellow rust.

#### ***4.4 Implications for breeding***

During the last decades, remote sensing approaches for in-field-detection of the symptoms of pathogenic fungi have received increased attention (Fiorani et al., 2012). Among these approaches, multi- and hyper-spectral sensing and imagery and chlorophyll fluorescence have been proposed (Fiorani et al., 2012; Franke et al., 2005). However, spectroradiometry and even more multi- and hyper-spectral imagery and fluorescence imagery are expensive and mostly focused in assessing individual leaves rather than canopies (Bock et al., 2010). For example whereas commercial systems of fluorescence imaging have been applied to monitor effects of plant pathogens (e.g. rust) in wheat (Bürling et al., 2011; Kuckenberg et al., 2008, 2009), most of them are limited to the level of single leaves because the difficulty of applying homogeneous and high-light conditions needed to probe the photosynthetic apparatus of whole shoots at larger (canopy in the field) scales (Fiorani et al., 2012). However, as explained above, the RGB images are easy and fast to acquire under field conditions (only a conventional RGB camera under sunlight is required) and data analysis is highthroughput using open access software (Casadesus et al., 2007; Casadesus and Villegas, 2014). According to previous experiments under different water regimes, the color components of  $H$ ,  $GGF$  and  $GF$  combined with  $a$  and  $u$  were effective in estimating the leaf area index and plant aerial biomass (Casadesús et al., 2005, 2007, 2014). In our study PCA at grain filling placed GY,  $H$ ,  $GF$ , and  $GGF$  in close proximity, and opposite to  $a$  and  $u$  on the same axis. Therefore, all these color

parameters may be considered as picture-derived vegetation indices (picVIs) reflecting genotypic variability of green vegetation under yellow rust infection. Other color components such as  $L$ ,  $I$ , which correspond to images obtained by the camera's self-adjustment to lighting environments, did not perform well as vegetation indices (Casades ús et al., 2005, 2007, 2014). Overall, the color parameters  $H$ ,  $a$ ,  $u$ ,  $GF$  and  $GGF$  performed better than the set of physiological traits ( $Chl$ ,  $P_n$ ,  $g_s$ ,  $E$  and  $CTD$ ) in evaluating grain yield and susceptibility to yellow rust. The results of this study demonstrate that RBG images appear as a low-cost and effective approach to evaluate genotypic resistance to yellow rust. Moreover, our study gives experimental support to previous work (Robert et al., 2004, 2005; Carretero et al., 2011) that concluded that the key variable for estimating rust damage (either directly or through a crop growth model targeted to assess both epidemiology and crop loss) is the total visible diseased area.

**Acknowledgements:** We acknowledge to Dr. Jaume Casades ús for kindly providing the BreedPix program. This work was supported by the project AGL2013-44147 from the Ministerio de Econom ía y Competitividad, Spain.

## References

- Akfirat F., Aydin Y., Ertugrul F., Hasancebi S., Budak H., Akan K., Mert Z., Bolat N., Uncuoglu A., 2010. A microsatellite marker for yellow rust resistance in wheat. **Cereal Research Communications** 38, 203-210.
- Aparicio, N., Villegas, D., Casadesus, J., Araus, J.L., Royo, C., 2000. Spectral Vegetation Indices as Nondestructive Tools for Determining Durum Wheat Yield. **Agronomy Journal** 92, 83-91.
- Araus J.L., Cairns J.E., 2014. Field high-throughput phenotyping: the new crop breeding frontier. **Trends in Plant Science** 19, 52-61.
- Arregui L.M., Lasa B., Lafarga A., Irañeta I., Baroja E., Quemada M., 2006. Evaluation of chlorophyll meters as tools for N fertilization in winter wheat under humid Mediterranean conditions. **European Journal of Agronomy** 24, 140-148.
- Ashourloo D., Mobasheri M.R., Huete A., 2014. Evaluating the effect of different wheat rust disease symptoms on vegetation indices using hyperspectral measurements. **Remote Sensing** 6, 5107-5123.
- Berghaus R., Reisener H.J., 1985. Changes in photosynthesis of wheat plants infected with wheat stem rust (*Puccinia graminis* f. sp. *tritici*). **Journal of Phytopathology**

112, 165-172.

Bethenod O., Huber L., Slimi H., 2001. Photosynthetic response of wheat to stress induced by *Puccinia recondita* and post-infection drought. **Photosynthetica** 39, 581-590.

Bock, C.H., Poole, G.H., Parker, P.E., Gottwald, T.R., 2010. Plant Disease Severity Estimated Visually, by Digital Photography and Image Analysis, and by Hyperspectral Imaging. **Critical Reviews in Plant Sciences** 29, 59-107.

Bürling, K., Hunsche, M., Noga, G., 2011. Use of blue-green and chlorophyll fluorescence measurements for differentiation between nitrogen deficiency and pathogen infection in winter wheat. **Journal of Plant Physiology** 168, 1641-1648.

Cabrera-Bosquet L., Crossa J., von Zitzewitz J., Serret M.D., Araus J.L., 2012. High-throughput phenotyping and genomic selection: the frontiers of crop breeding converge. **Journal of Integrative Plant Biology** 54, 312-320.

Carretero R., Bancal M.O., Miralles D.J., 2011. Effect of leaf rust (*Puccinia triticina*) on photosynthesis and related processes of leaves in wheat crops grown at two contrasting sites and with different nitrogen levels. **European Journal of Agronomy** 35, 237-246.

Casadesús J., Biel C., Savé R., 2005. Turf color measurement with conventional digital cameras. In Proceedings of 2005 EFITA/WCCA Joint Congress on IT in Agriculture, pp. 804–811. Vila Real, Portugal: Universidade de Trás-os-Montes e Alto Douro.

Casadesús J., Kaya Y., Bort J., Nachit M.M., Araus J.L., Amor S., Ferrazzano G., Maalouf F., Maccaferri M., Martos V., Ouabbou H., Villegas D., 2007 Using vegetation indices derived from conventional digital cameras as selection criteria for wheat breeding in water-limited environments. **Annals of Applied Biology** 150, 227-236.

Casadesús J., Villegas D., 2014. Conventional digital cameras as a tool for assessing leaf area index and biomass for cereal breeding. **Journal of Integrative Plant Biology** 56, 7-14.

Chen X., Moore M., Milus E.A., Long D.L., Line R.F., Marshall D., Jackson L., 2002. Wheat stripe rust epidemics and races of *Puccinia striiformis* f. sp. *tritici* in the United States in 2000. **Plant Disease** 86, 39-46.

Cheng H.D., Jiang X.H., Sun Y., Wang J., 2001. Color image segmentation: advances and prospects. **Pattern Recognition** 34, 2259-2281.

Devadas R., Lamb D.W., Simpfendorfer S., Backhouse D., 2009. Evaluating ten spectral vegetation indices for identifying rust infection in individual wheat leaves. **Precision Agriculture** 10, 459-470.

Diéguez-Uribeondo, J., Förster, H., Adaskaveg, J.E., 2003. Digital image analysis of

internal light spots of appressoria of *Colletotrichum acutatum*. **Phytopathology** 93, 923–930.

Fiorani, F., Rascher, U., Jahnke, S., Schurr, U., 2012. Imaging plants dynamics in heterogenic environments. **Current Opinion in Biotechnology** 23, 227-235.

Franke, J., Menz, G., Oerke, E.-C., Rascher, U., 2005. Comparison of multi- and hyperspectral imaging data of leaf rust infected wheat plants, pp. 59761D-59761D-59711.

Gooding M.J., Dimmock J.P.R.E., France J., Jones S.A., 2000. Green leaf area decline of wheat flag leaves: the influence of fungicides and relationships with mean grain weight and grain yield. **Annals of Applied Biology** 136, 77-84.

Graeff S., Link J., Claupein W., 2006. Identification of powdery mildew (*Erysiphe graminis* sp. *tritici*) and take-all disease (*Gaeumannomyces graminis* sp. *tritici*) in wheat (*Triticum aestivum* L.) by means of leaf reflectance measurements. **Central European Journal of Biology** 1, 275-288.

Han D.J., Wang Q.L., Zhang L., Wei G.R., Zeng Q.D., Zhao J., Wang X.J., Huang L.L., Kang Z.S., 2010. Evaluation of resistance of current wheat cultivars to stripe rust in northwest China, north China and the middle and lower reaches of Changjiang river epidemic area. **Scientia Agricultura Sinica** 43, 2889-2896. (Chinese version with English abstract)

He Z., Xia X., Chen X., Zhuang Q., 2011. Progress of wheat breeding in China and the future perspective. **Acta Agronomica Sinica** 37, 202-215. (Chinese version with English abstract)

Herrera-Foessel S.A., Singh R.P., Huerta-Espino J., Crossa J., Yuen J., Djurle A., 2006. Effect of leaf rust on grain yield and yield traits of durum wheats with race-specific and slow-rusting resistance to leaf rust. **Plant Disease** 90, 1065-1072.

Karcher D.E., Richardson M.D., 2005. Batch Analysis of Digital Images to Evaluate Turfgrass Characteristics. **Crop Science** 45, 1536-1539.

Kipp S., Mistele B., Schmidhalter U., 2014. Identification of stay-green and early senescence phenotypes in high-yielding winter wheat, and their relationship to grain yield and grain protein concentration using high-throughput phenotyping techniques. **Functional Plant Biology** 41, 227-235.

Kolmer J.A., Singh R.P., Garvin D.F., Viccars L., William H.M., Huerta-Espino J., Ogbonnaya F.C., Raman H., Orford S., Bariana H.S., Lagudah E.S., 2008. Analysis of the Lr34/Yr18 Rust Resistance Region in Wheat Germplasm. **Crop Science** 48, 1841-1852.

Kuckenbergl J., Tartachnyk I., Noga G., 2009. Detection and differentiation of nitrogen-deficiency, powdery mildew and leaf rust at wheat leaf and canopy level by laser-induced chlorophyll fluorescence. **Biosystems Engineering** 103, 121-128.

Kuckenberg, J., Tartachnyk, I., Noga, G., 2008. Temporal and spatial changes of chlorophyll fluorescence as a basis for early and precise detection of leaf rust and powdery mildew infections in wheat leaves. **Precision Agriculture** 10, 34-44.

Kurniawati N.N., Abdullah S.N.H.S., Abdullah S., Abdullah S., 2009. Investigation on image processing techniques for diagnosing paddy diseases. In *Soft Computing and Pattern Recognition*, 2009, pp. 272-277 SOCPAR International Conference.

Lenthe J.H., Oerke E.C., Dehne H.W., 2007. Digital infrared thermography for monitoring canopy health of wheat. **Precision Agriculture** 8, 15-26.

Lukina E.V., Stone M.L., Raun W.R., 1999. Estimating vegetation coverage in wheat using digital images. **Journal of Plant Nutrition** 22, 341-350.

McGrath M.T., Pennypacker S.P., 1990. Alteration of physiological processes in wheat flag leaves caused by stem rust and leaf rust. **Phytopathology** 80, 677-686.

Mirik M., Michels G.J., Kassymzhanova-Mirik S., Elliott N.C., Catana V., Jones D.B., Bowling R., 2006. Using digital image analysis and spectral reflectance data to quantify damage by greenbug (Hemiptera: Aphididae) in winter wheat. **Computers and Electronics in Agriculture** 51, 86-98.

Moshou, D., Bravo, C., West, J., Wahlen, S., McCartney, A., Ramon, H., 2004. Automatic detection of 'yellow rust' in wheat using reflectance measurements and neural networks. **Computers and Electronics in Agriculture** 44, 173-188.

Munns R., James R.A., Sirault X.R.R., Furbank R.T., Jones H.G., 2010. New phenotyping methods for screening wheat and barley for beneficial responses to water deficit. **Journal of Experimental Botany** 61, 3499-3507.

Pan G., Li F.M., Sun G.J., 2007. Digital camera based measurement of crop cover for wheat yield prediction. In *Geoscience and Remote Sensing Symposium*, pp. 797-800 IGARSS 2007, IEEE International.

Reyniers M., Vrindts E., Baerdemaeker J.D., 2004. Optical measurement of crop cover for yield prediction of wheat. **Biosystems Engineering** 89, 383-394.

Robert C., Bancal M.O., Ney B., Lannou C., 2005. Wheat leaf photosynthesis loss due to leaf rust, with respect to lesion development and leaf nitrogen status. **New Phytologist** 165, 227-241.

Robert C., Bancal M.O., Nicolas P., Lannou C., Ney B., 2004. Analysis and modelling of effects of leaf rust and *Septoria tritici* blotch on wheat growth. **Journal of Experimental Botany** 55, 1079-1094.

Römer C., Wahabzada M., Ballvora A., Pinto F., Rossini M., Panigada C., Behmann J., León J., Thurau C., Bauckhage C., Kersting K., Rascher U., Plümer L., 2012. Early drought stress detection in cereals: simplex volume maximisation for hyperspectral image analysis. **Functional Plant Biology** 39, 878-890.

Rosewarne G.M., Singh R.P., Huerta-Espino J., William H.M., Bouchet S., Cloutier S., McFadden H., Lagudah E.S., 2006. Leaf tip necrosis, molecular markers and  $\beta$ 1-proteasome subunits associated with the slow rusting resistance genes Lr46/Yr29. **Theoretical and Applied Genetics** 112, 500-508.

Scholes J., Rolfe S., 1996. Photosynthesis in localised regions of oat leaves infected with crown rust ( *Puccinia coronata* ): quantitative imaging of chlorophyll fluorescence. **Planta** 199, 573-582.

Scholes J.D., Lee P.J., Horton P., Lewis D.H., 1994. Invertase: understanding changes in the photosynthetic and carbohydrate metabolism of barley leaves infected with powdery mildew. **New Phytologist** 126, 213-222.

Singh R.P., Nelson J.C., Sorrells M.E., 2000. Mapping Yr28 and other genes for resistance to stripe rust in wheat. **Crop Science** 40, 1148-1155.

Smith, R.C.G., Heritage, A.D., Stapper, M., Barrs, H.D., 1986. Effect of stripe rust (*puccinia striiformis* west.) and irrigation on the yield and foliage temperature of wheat. **Field Crops Research** 14, 39-51.

Spitters C.J.T., Van Roermund H.J.W., Van Nassau H.G.M.G., Schepers J., Mesdag J., 1990. Genetic variation in partial resistance to leaf rust in winter wheat: disease progress, foliage senescence and yield reduction. **Netherlands Journal of Plant Pathology** 96, 3-15.

Teena M., Manickavasagan A., 2014. Thermal Infrared Imaging. In: Imaging with Electromagnetic Spectrum, pp. 147-173 Eds A. Manickavasagan and H. Jayasuriya. Heidelberg, Berlin, Germany: Springer.

Trethowan R.M., Reynolds M., Sayre K., Ortiz-Monasterio I., 2005. Adapting wheat cultivars to resource conserving farming practices and human nutritional needs. **Annals of Applied Biology** 146, 405-413.

Trussell H.J., Vrhel M.J., Saber E., 2005. Color image processing. **IEEE Signal Processing Magazine** 22, 14-22.

Wan A.M., Chen X.M., He Z.H., 2007. Wheat stripe rust in China. **Australian Journal of Agricultural Research** 58, 605-619.

Yang Z., Rao M.N., Elliott N.C., Kindler S.D., Popham T.W., 2009. Differentiating stress induced by greenbugs and Russian wheat aphids in wheat using remote sensing. **Computers and Electronics in Agriculture** 67, 64-70.

Yin G.H., Wang J.W., Wen W.E., He Z.H., Li Z.F., Wang H., Xia X.C., 2009. Mapping of wheat stripe rust resistance gene YrZH84 with RGAP markers and its application. **Acta Agronomica Sinica** 35, 1274-1281.

Zeng S. M., Luo Y., 2008. Systems analysis of wheat stripe rust epidemics in China. **European Journal of Plant Pathology** 121, 425-438.

	<i>I</i>	<i>H</i>	<i>S</i>	<i>L</i>	<i>a</i>	<i>b</i>	<i>u</i>	<i>v</i>	<i>GF</i>	<i>GGF</i>
Lankao 298	0.30 a	42.82 g	0.29 b	36.21 a	-2.24 a	22.42 cd	6.88 a	22.75 b	0.13 f	0.03 f
Lankao 198	0.30 a	46.26 g	0.33 a	37.45 a	-3.53 a	25.67 ab	6.34 a	25.90 ab	0.16 f	0.04 f
Lankao 282	0.29 a	54.70 f	0.35 a	36.48 a	-6.97 b	26.36 a	1.88 b	26.75 a	0.43 e	0.08 f
Lankao 223	0.27 a	66.08 cd	0.26 bc	34.56 a	-9.39 cd	21.40 d	-2.87 de	22.74 b	0.70 bcd	0.38 cd
Aikang 58	0.29 a	57.46 ef	0.28 b	36.73 a	-7.53 bc	23.26 bcd	0.20 bc	24.54 ab	0.49 e	0.17 ef
Yumai 66	0.29 a	65.41 cde	0.23 c	36.82 a	-8.98 bcd	20.55 d	-2.58 cde	22.57 b	0.67 cd	0.37 cd
Zhoumai 25	0.30 a	58.05 def	0.28 b	38.80 a	-8.10 bc	24.41 abc	-0.10 bcd	26.16 ab	0.58 de	0.26 de
Lankao 0347	0.31 a	71.78 bc	0.24 bc	36.41 a	-11.10 ef	21.73 cd	-4.86 efg	23.83 ab	0.83 ab	0.54 abc
Gazul	0.28 a	79.76 ab	0.23 c	36.24 a	-12.66 fg	20.96 d	-7.05 gh	23.42 ab	0.84 ab	0.65 ab
Arthur Nick	0.28 a	77.89 ab	0.22 c	35.98 a	-11.83 fg	20.27 d	-6.25 fgh	22.61 b	0.86 ab	0.67 ab
Zhoumai 18	0.29 a	67.91 c	0.26 bc	36.89 a	-10.48 ef	22.61 cd	-3.80 ef	24.56 ab	0.79 abc	0.50 bc
Zhoumai 22	0.30 a	80.89 a	0.23 c	38.21 a	-13.59 g	22.01 cd	-7.94 h	24.99 ab	0.91 a	0.70 a

Table S1. Mean values of color parameters of twelve different wheat genotypes during grain filling infected by yellow rust under field conditions. Footnote<sup>6</sup>

<sup>6</sup> The color parameters represent the average color components of the whole image expressed in the color spaces of Intensity, Hue and Saturation (*H*, *I* and *S*), CIELab (*L*, *a* and *b*) and CIELuv (*L*, *u* and *v*). *GF* is the relative green fraction of the image and *GGF* is the relative greener fraction from *H* histograms. For each genotype and trait values are the means of 3 replicates. All genotypes were listed according grain yield from low (upper) to high (lower row) according Table 1.

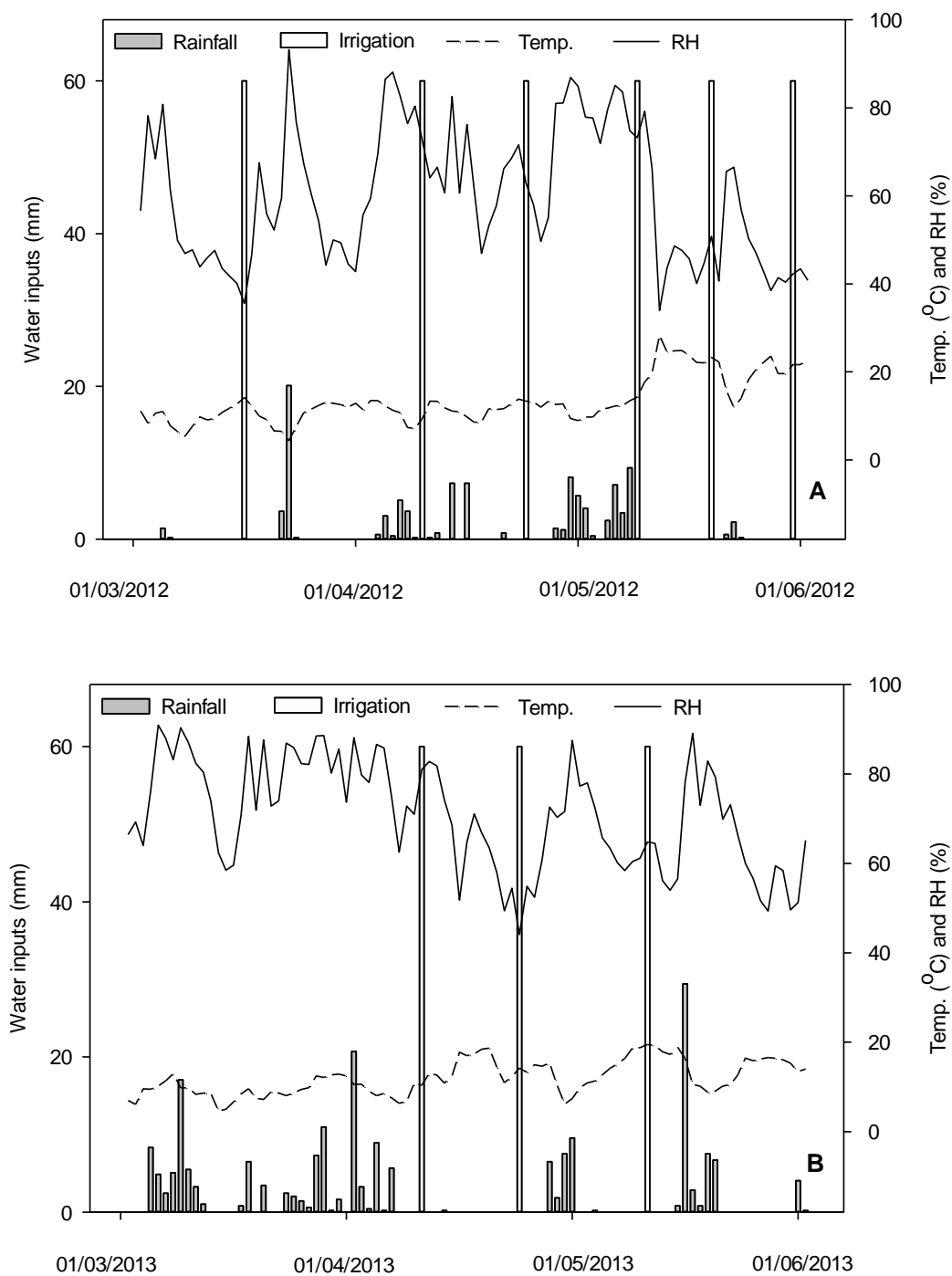


Figure S1. Water inputs of daily mean rainfall (rainfall), support irrigation (irrigation), and daily mean air temperature (temp.) and relative humidity (RH) from 1<sup>st</sup> of March to 1<sup>st</sup> of June during the growing season 2011-2012 (A) and 2012-2013(B) at the Aranjuez Experimental Station (Madrid Province, Spain).